Estimating Contemporary and Future Wind-Damage Losses from Hurricanes Affecting Eglin Air Force Base, Florida

JAMES B. ELSNER, SHAWN W. LEWERS, JILL C. MALMSTADT, AND THOMAS H. JAGGER

Department of Geography, The Florida State University, Tallahassee, Florida

(Manuscript received 20 September 2010, in final form 21 February 2011)

ABSTRACT

The strongest hurricanes over the North Atlantic Ocean are getting stronger, with the increase related to rising ocean temperature. Here, the authors develop a procedure for estimating future wind losses from hurricanes and apply it to Eglin Air Force Base along the northern coast of Florida. The method combines models of the statistical distributions for extreme wind speed and average sea surface temperature over the Gulf of Mexico with dynamical models for tropical cyclone wind fields and damage losses. Results show that the 1-in-100-yr hurricane from the twentieth century picked at random to occur in the year 2100 would result in wind damage that is 36% [(13%, 76%) = 90% confidence interval] greater solely as a consequence of the projected warmer waters in the Gulf of Mexico. The method can be applied elsewhere along the coast with modeling assumptions modified for regional conditions.

1. Introduction

Hurricanes and tropical storms pose a serious natural threat to coastal military infrastructure. High wind, storm surge, and rainfall flooding can cause significant damage. Since 2005, the United States has experienced devastating impacts from strong hurricanes, including Katrina, Rita, Wilma, and Ike. Research indicates that as ocean temperatures have risen the strongest hurricanes have gotten stronger (Elsner et al. 2008b). These increases are likely to continue with rising global temperatures (Knutson et al. 2010; Bender et al. 2010).

Hurricane hazard models are valuable for estimating contemporary wind-damage losses to buildings and infrastructure, and they are widely used for insurance rate adjustments in government and private industry. At present, the models do not incorporate the potential effects of climate variability and climate change, however. Here, we propose a method that makes use of components of a hazard model in conjunction with statistical models of tropical cyclone trends to estimate future wind-damage losses. We develop the method for the Eglin Air Force Base (EAFB), which is located in the Florida Panhandle, but it is general enough that it can be applied to other coastal locations.

EAFB is used by the U.S. military as a development and testing ground for air-delivered weaponry. The military has invested millions of dollars in infrastructure on the base, ranging from roads and air fields to personnel housing and radar installations. Given its proximity to the Gulf of Mexico, much of this built environment is exposed to hurricane winds. In particular, military planners are concerned with the potential increasing risk of wind-damage and surge losses under future climate scenarios.

We first investigate the contemporary hurricane wind risk to EAFB by using a wind-field model on historical hurricanes that have affected the region and by statistically modeling the resulting local wind speeds. We then attempt to estimate the future wind risk by considering an adjustment to the intensity of the strongest hurricanes. The adjustment is based on the nonlinear statistical relationship between hurricane intensity and sea surface temperature (SST) and a linear trend in SST. Our analysis shows that, if future projections of hurricane intensity are realized, coastal losses on the 1-in-100-yr (1 in 500 yr) storm will increase by 36% (52%) relative to today's losses, making EAFB more vulnerable to future losses from the strongest hurricanes. The greater vulnerability arises from increases in the intensity of the strongest hurricanes.

We begin in section 2 with a summary of the hurricanes that have affected EAFB. We describe the available datasets and the procedure for identifying hurricanes from

Corresponding author address: James B. Elsner, Dept. of Geography, The Florida State University, Tallahassee, FL 32301.
E-mail: jelsner@fsu.edu

DOI: 10.1175/2011JAMC2658.1

the past for this analysis. The frequency, track, and intensity of the historical hurricanes are displayed. In section 3, we examine the procedures for estimating contemporary wind losses with the use of the multihazard version of the "HAZUS" hurricane hazard model (HAZUS-MH, hereinafter referred to as HAZUS) and a postprocessing of the output using extreme-value statistics. In section 4, we model the recent changes in hurricane intensity for storms over the Gulf of Mexico. In section 5, we model the rising trend in SST, and in section 6, we combine the two models to project tropical cyclone intensities to 2100. In section 7, we use our modeled estimates of future hurricane intensities to compare the projected relative increase in wind-damage losses 90 yr from now. We provide a summary and list model limitations in section 8.

2. Past hurricanes that have affected EAFB

a. Data

We begin by considering the historical record of hurricanes having a wind impact on EAFB. The data come from the National Hurricane Center's Hurricane Database (HURDAT, or best track; Landsea et al. 2004). This is the official record of tropical cyclones for the Atlantic Ocean, Gulf of Mexico, and Caribbean Sea, including those that have made landfall in the United States. The record consists of the 6-hourly cyclone location and intensity for individual storms back to 1851 and was originally assembled in the 1960s to support the objectives of the National Aeronautics and Space Administration Apollo spaceflight program because launches were conducted along Florida's hurricane-vulnerable east coast. The precision of the data that make up HURDAT has increased as analysis techniques and understanding of hurricanes have improved over time.

The data are widely used in research on hurricanes, including studies on the seasonal predictability of hurricanes across the Atlantic (Klotzbach 2008) and along the U.S. coastline (Elsner and Jagger 2004) and studies on climate variability and climate change (Kossin and Camargo 2009; Elsner et al. 2008a). Yet, the data contain random errors and systematic biases introduced by the improved accuracy of records over time. Identification and removal of these errors as well as ways to treat the systematic biases are on going (Landsea et al. 2004; Vecchi and Knutson 2008; Solow 2010; Landsea et al. 2010). Although the quantitative loss results presented in this paper will certainly be affected by future improvements to the dataset, our purpose here is to demonstrate a method for estimating future losses. Although we show that hurricane data biases over the twentieth century do not significantly affect our trend results, success at demonstrating the method should be judged separately from opinions about how data inhomogeneities and random errors might modify the conclusions. Moreover, it should be kept in mind that the data are the most consistent source of information on past hurricanes that is available and that our analysis focuses on hurricanes near the Gulf coast, where storm records are more reliable than those over the open ocean.

b. Procedure for selecting hurricanes

For use in this study, the best-track tropical cyclone data were interpolated hourly for the geographic position of the center fix and wind speed using a polynomial (of degree 3) smoother that was described in Jagger and Elsner (2006). The spline smoothing uses three points to the left and two to the right along with the current value to preserve the 6-hourly wind speed and to provide an interpolation of values at each hour between those values. The spline fit is performed using the method of least squares.

All tropical cyclones passing within 140 km (great circle distance) of the point 30.4°N, 86.8°W over the period 1851–2009 that had wind speeds exceeding the hurricane threshold (33 m s^{-1}) within this distance are considered for this study. The point is located on Santa Rosa Island, approximately 30 km southwest of the geographic center of EAFB. A hurricane making landfall here places much of the EAFB in the most destructive (right) side (relative to the direction of motion) of the storm (Scheitlin et al. 2011). The 140-km radius is one-half of the typical width of the swath of hurricane-force winds for hurricanes that exceed 50 m s^{-1} as determined on the basis of a hurricane-strike model developed by Keim et al. (2007).

Note that our interest is in wind damage. Large (and even some medium sized) hurricanes outside our search radius could produce a damaging surge at coastal locations on EAFB but are not considered here. For instance Hurricane Katrina (2005), in making landfall on the Louisiana–Mississippi border more than 250 km to the west of our fiducial point, produced a surge on portions of Santa Rosa Island that exceeded 1.5 m, but Katrina's winds are not included in our analysis and modeling because they did not exceed tropical-storm force in this region (Barnett 2006).

The search that was based on the above criteria returned 39 hurricanes that occurred over the period 1851–2009. This amounts to an overall mean of 0.24 hurricanes per year or about 1 hurricane every 4 yr. The frequencies, tracks, and intensities of the EAFB hurricanes are shown in Fig. 1. The longest period without a hurricane lasted 18 yr, from 1957 through 1974. The annual variance is 0.24 (hurricanes per year)$^{-2}$, which is

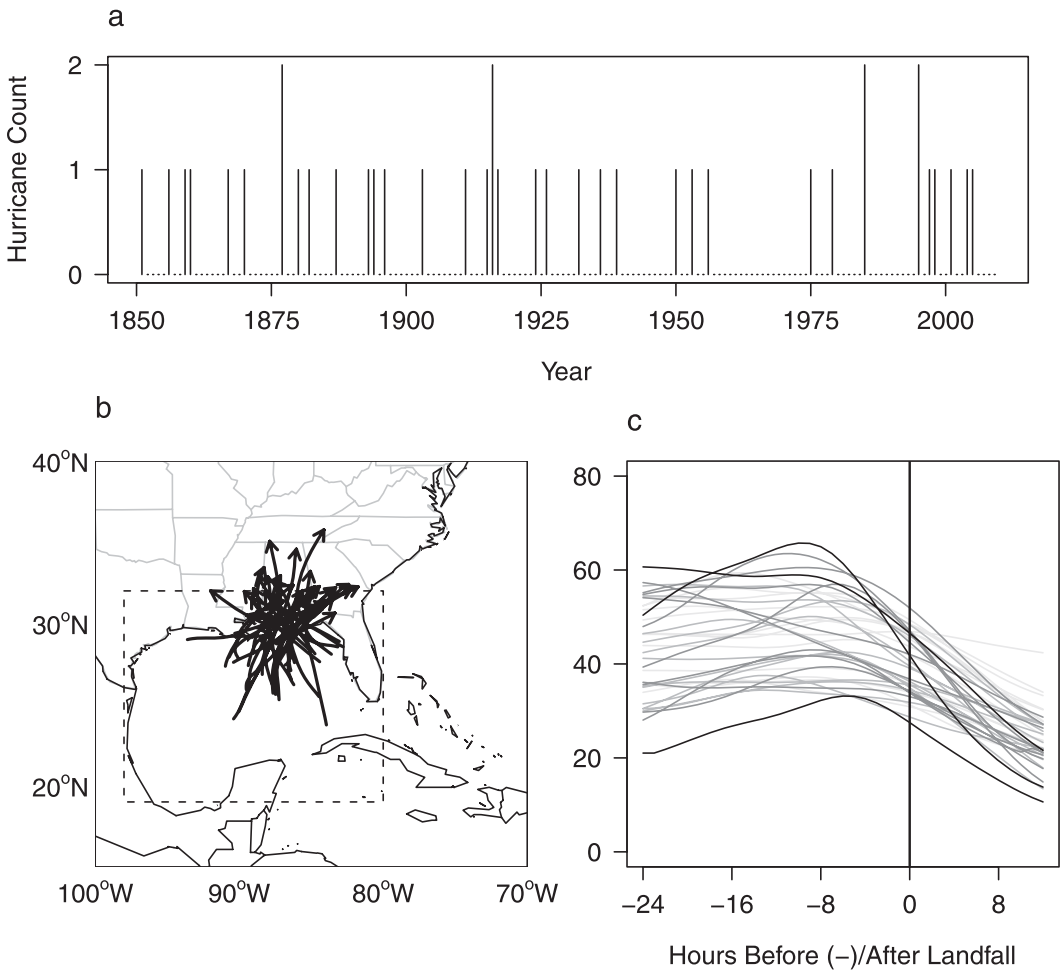

FIG. 1. Hurricanes that have affected EAFB. (a) Occurrences of the 39 tropical cyclones that have come within 140 km of Santa Rosa Island (30.4°N, 86.8°W) with winds of at least hurricane speed (33 m s^{-1}). (b) Track positions 24 h before and 12 h after landfall for all of the hurricanes. (c) The maximum wind speeds (m s^{-1}) of each of the tropical cyclones relative to landfall. The landfall time is shown with a vertical line. The gray shading in the wind speed intensity profiles indicates time periods, with the darkest gray indicating the most recent hurricanes (after the year 2000).

consistent with the annual counts being a Poisson process in which the mean and the variance are the same. Assuming a Poisson rate equal to the overall mean, the chance of no hurricanes affecting the base over an 18-yr stretch is 1.3%. There are four years with a two-hurricane impact, with the most recent occurring in 1995. There is no significant upward or downward trend in the frequency of hurricanes affecting EAFB. This is consistent with modeling studies that show global frequency either decreasing or remaining essentially unchanged as a result of ''greenhouse'' warming (Knutson et al. 2010).

The landfall point is the closest hourly-interpolated location to land. The entire set of track locations and wind speeds is truncated to include only locations 24 h before and 12 h after landfall, for a total of 37 h (including the landfall point) for each track. The hurricane of 1870 is removed from further analysis (although it counts in the frequency statistic) because it contains only a single track point. Hurricanes tend to approach EAFB from the southwest, south, and southeast with equal regularity, and it is just as likely for a hurricane to pass to the east of EAFB as to the west.

The hurricane intensities along the track segment before and after landfall are shown in Fig. 1. The gray shading indicates time periods, with the darkest gray indicating the hurricanes since 2000. In general, the historical hurricanes intensify as they approach the coast and then begin to decay 6–9 h prior to landfall. The weakening of winds prior to landfall is likely related to the hurricane ingesting dry, aerosol-laden air from the

continent (Khain et al. 2010) as well as to hurricane-induced cooling of the sea surface (Rappaport et al. 2010). The strongest hurricanes tend to decay faster once over land, and there is an upward trend in the intensity of hurricanes approaching EAFB (Malmstadt et al. 2009).

c. Hurricane characteristics along the track

The set of historical hurricanes provides a sample of storms from which wind-damage losses will be estimated using the HAZUS hurricane model (Vickery et al. 2009a). Additional information beyond the hurricane track and maximum wind speeds is necessary as input to the hurricane model. This information includes forward speed, radius to maximum winds, the Holland B parameter, minimum central pressure, and a binary variable indicating whether the storm is over land or water.

The total damage from a hurricane at a given location also depends on how long the wind blows, which is a function of the hurricane's forward speed and size. A hurricane moving slower over an area will cause more damage than a hurricane moving faster, all else being equal. According to Scheitlin et al. (2011), hurricanes approaching EAFB move at speeds of 6–7 m s^{-1} on average, with a slight acceleration prior to landfall. After landfall, there is a significant increase in forward velocity as the hurricanes get pushed northward and eastward under the influence of the midlatitude jet streams. Here, the forward speed in units of knots is computed from the change in location of the center fixes at hourly intervals.

Hurricane wind speeds increase from near zero inside the eye to a maximum in the eyewall and then decrease outward. The average distance from the storm center to the circle of maximum wind speed is called the radius to maximum winds R_{MW} and is adopted as a convenient parameter to be used as the size or lateral extent of the hurricane. The R_{MW} determines the spatial extent of the hurricane force winds and determines, along with forward speed, how long a given location experiences these forces. We use the landfall R_{MW} values from the HURDAT metadata for all locations along the track for hurricanes after 1900, with the exception of the storm in 1915 and Hurricane Barry in 2001. For the balance of hurricanes, we use the average $R_{MW} = 40$ km that is computed from hurricanes with size information. All R_{MW} values are held constant along the track segment.

The decrease of wind speeds outside the R_{MW} is described by the Holland B parameter (Holland 1980). The Holland B parameter is a nondimensional value ranging between 1 and 2.5 that expresses the weakening of wind speeds (decay rate) as a function of distance from R_{MW}. A lower Holland B value indicates a slower decay rate, indicating a larger region of high wind winds. For specifying the Holland B along the historical tracks we use the empirical formula of Vickery and Wadhera (2008), which is based on R_{MW} and the center-fix latitude.

We get minimum central pressure values from the empirical wind–pressure relationship of Brown et al. (2006) for Gulf of Mexico hurricanes. The relationship describes how wind speeds are related to minimum central pressures, with faster winds associated with lower minimum pressures.

Table 1 lists the hourly interpolated and corresponding characteristic values for Hurricane Eloise of 1975. Eloise approached EAFB from the south on 22 September and made landfall a day later. Eloise had an estimated minimum central pressure of 927 hPa 6 h prior to landfall. Landfall pressure is estimated at 952 hPa. The storm had a radius to maximum winds of 26 km and an initial forward speed of about 4 m s^{-1} that increased to 16 m s^{-1} shortly after landfall. These sets of values are considered to be the "storm vitals" because they are used as input to the HAZUS model.

d. Hurricane wind-field model

The wind speed attached to each track point in the storm vitals represents the fastest wind somewhere within the hurricane. To get the fastest wind speed at any geographic location from a particular storm, we use a hurricane wind-field model. The wind-field model used here is part of the HAZUS hurricane hazard model that mathematically simulates hurricane wind speeds for the purpose of estimating local wind risk for the design and assessment of loads to structures. The model is described in detail in Vickery et al. (2009b).

In brief, the model first generates a spatial wind field at gradient height from each set of storm vitals along the historical track using the gradient wind relationship. Next, the gradient wind speed is adjusted to mean near-surface (e.g., 10-m height) wind speed assuming neutral stability in the atmospheric boundary layer. Third, the mean wind speeds are adjusted on the basis of local terrain specified from land-use land-cover maps using gust factors. Greater friction associated with a rougher land surface causes a weakening of the average wind speeds. A time trace of the wind speed at any location of interest allows us to get the highest local gust velocity.

We compare the HAZUS-generated wind speeds at the centroids of the six census tracts composing EAFB with corresponding wind speeds from the Hurricane Wind Analysis System (H*Wind; Powell et al. 1998) for Hurricanes Ivan (2004) and Dennis (2005). The H*Wind values are from a temporal sequence of wind-field "snapshots" as the hurricane moves onshore. Each snapshot is

TABLE 1. Storm vitals for Hurricane Eloise of 1975. The latitude ϕ and longitude λ in decimal degrees are those of the equal-interval points along the track. The time is in UTC. The wind speed w (m s^{-1}), translation speed s (m s^{-1}), radius to maximum winds R_{MW} (km), minimum central pressure p (hPa), and Holland B parameter are from the extended best-track data. The column that is labeled ''Inland'' is a binary variable indicating whether the storm location is over water (0) or land (1).

Date	Time	λ	ϕ	w	p	R_{MW}	Holland B	s	Inland
22 Sep	1300	−89.51	25.93	39.3	968	26	1.33	3.9	0
22 Sep	1400	−89.51	26.05	40.2	966	26	1.33	3.6	0
22 Sep	1500	−89.51	26.17	41.1	964	26	1.33	3.5	0
22 Sep	1600	−89.50	26.28	42.0	962	26	1.33	3.5	0
22 Sep	1700	−89.46	26.39	42.8	960	26	1.32	3.7	0
22 Sep	1800	−89.40	26.50	43.6	959	26	1.32	4.3	0
22 Sep	1900	−89.31	26.62	44.5	957	26	1.32	4.8	0
22 Sep	2000	−89.18	26.74	45.1	955	26	1.32	5.4	0
22 Sep	2100	−89.04	26.87	45.9	954	26	1.32	6.0	0
22 Sep	2200	−88.87	27.01	46.8	952	26	1.32	6.4	0
22 Sep	2300	−88.69	27.15	47.9	949	26	1.31	6.8	0
23 Sep	0000	−88.50	27.30	49.2	946	26	1.31	7.1	0
23 Sep	0100	−88.30	27.46	50.7	943	26	1.31	7.3	0
23 Sep	0200	−88.11	27.62	52.3	939	26	1.31	7.6	0
23 Sep	0300	−87.90	27.80	53.9	935	26	1.31	7.8	0
23 Sep	0400	−87.70	27.98	55.3	931	26	1.30	8.1	0
23 Sep	0500	−87.50	28.18	56.4	928	26	1.30	8.5	0
23 Sep	0600	−87.30	28.40	57.0	927	26	1.30	8.8	0
23 Sep	0700	−87.10	28.64	56.9	927	26	1.30	9.2	0
23 Sep	0800	−86.91	28.89	56.2	929	26	1.29	9.7	0
23 Sep	0900	−86.73	29.17	55.1	932	26	1.29	10.2	0
23 Sep	1000	−86.57	29.48	53.4	936	26	1.28	10.9	0
23 Sep	1100	−86.42	29.82	51.4	941	26	1.28	11.6	0
23 Sep	1200	−86.30	30.20	49.1	946	26	1.28	12.6	0
23 Sep	1300	−86.20	30.61	46.6	952	26	1.27	13.5	1
23 Sep	1400	−86.12	31.06	43.8	958	26	1.26	14.3	1
23 Sep	1500	−86.05	31.53	40.9	965	26	1.26	14.9	1
23 Sep	1600	−85.96	32.01	38.0	971	26	1.25	15.4	1
23 Sep	1700	−85.85	32.51	34.9	976	26	1.25	15.6	1
23 Sep	1800	−85.70	33.00	31.9	982	26	1.24	15.8	1
23 Sep	1900	−85.51	33.49	29.0	987	26	1.23	15.8	1
23 Sep	2000	−85.28	33.96	26.1	991	26	1.23	15.5	1
23 Sep	2100	−85.02	34.40	23.4	995	26	1.22	14.8	1
23 Sep	2200	−84.77	34.81	20.9	998	26	1.22	13.7	1
23 Sep	2300	−84.52	35.18	18.6	1001	26	1.21	12.2	1
24 Sep	0000	−84.30	35.50	16.6	1004	26	1.21	10.3	1
24 Sep	0100	−84.12	35.76	14.9	1005	26	1.20	8.4	1

gridded output from an objective analysis using all observations over a 4–6-h period. As part of the analysis system, data are quality controlled and processed to conform to a height of 10 m with an open-terrain exposure and with an averaging period of 1 min. We take the gridded values and use an inverse-distance weighting interpolation (30 nearest grid points) to estimate the wind speed at the census-tract centroids. The wind speed values are all within 2% of each other by varying the number of nearest points between 10 and 30. The H*Wind values are multiplied by 1.4 to get a 10-s gust consistent with the HAZUS wind-field values.

Figure 2 is a scatterplot of the H*Wind versus the HAZUS wind values in meters per second. The correspondence is excellent for Ivan and good for Dennis. HAZUS tends to overestimate the wind gusts when compared with H*Wind in Hurricane Dennis in regions of EAFB that experience weaker winds. At hurricane-intensity gusts (33 m s^{-1}), the overestimate is 18%. The correlation between winds from H*Wind and HAZUS for Ivan (Dennis) is 0.99 (0.95), indicating the HAZUS wind model matches the wind field of these historical hurricanes. The difference between the HAZUS-modeled and objectively analyzed H*Winds output results from the limits inherent in describing the wind field by single values of Holland B and R_{MW}, errors in modeling the atmospheric boundary layer, and errors in the height, terrain, and specifications of the storm vitals (Vickery et al. 2009b).

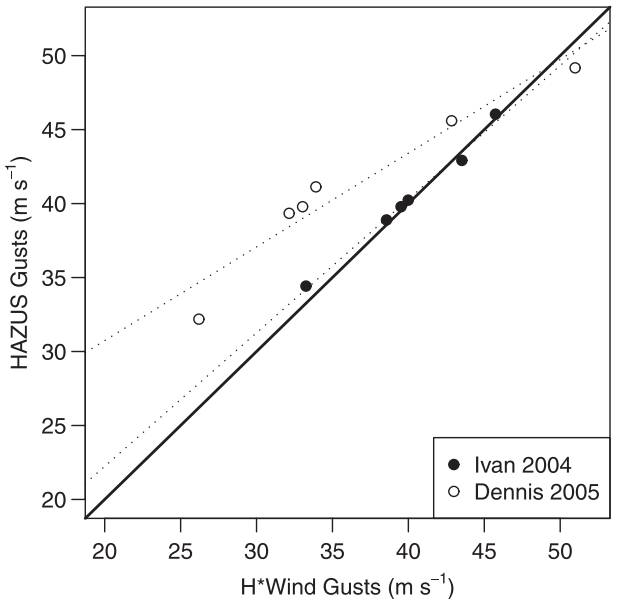

FIG. 2. H*Wind vs HAZUS wind speed gusts over EAFB for Hurricanes Ivan (2004) and Dennis (2005). The dotted lines are the regression lines that are based on the six census block values for each hurricane. The solid line shows $y = x$.

3. Contemporary wind speed and damage loss estimates

a. Wind speed exceedance probabilities

We input the storm vitals for each of the historical hurricanes and obtain the HAZUS-generated peak 10-s wind gusts at the geographic centroid of six census tracts. The set of historical local wind speed maxima at a given location is then modeled statistically using a peaks-over-threshold (POT) method (Elsner et al. 2008a; Malmstadt et al. 2010). The POT method estimates annual exceedance probabilities for given wind speeds. The statistical model is estimated for the winds at each of the census tracts independently. The exceedance probabilities represent the contemporary risk of hurricane winds affecting EAFB. Results of this procedure are shown in Fig. 3. The plots display the annual exceedance probability versus wind speeds for the six census tracts composing EAFB.

The plots are interpreted as follows. Considering the southernmost census tract, we can expect wind gusts of at least 40 m s^{-1} (exceedance level) at the centroid of the tract with an annual probability of slightly less than 10%. As hurricane intensity increases, annual probability decreases. The statistical model is shown by the solid curve, and the empirical estimates are shown with points. For consistency we use a threshold value of 33 m s^{-1} for the statistical model.

Empirical estimates are made using the annual probability, which is the product of the yearly hurricane rate times the exceedance probability. The yearly rate is the number of hurricanes divided by the record length in years. The exceedance probability for a particular wind speed is approximated by dividing the rank of the hurricane wind speed (the maximum gust has a rank of 1) in the record by the number of hurricanes after subtracting 0.5 from the rank. In general, the points fall close to the curves, indicating that the models fit the data well.

Results from our procedure compare favorably to the result that is based on a track-relative climatological model (Scheitlin et al. 2011), as shown by the red point and confidence interval for the southernmost tract. Census tracts farther from the coast have lower exceedance probabilities for given wind speeds. The wind speeds are based on the most recent 160 yr of climatological conditions, and therefore the plots represent contemporary estimates of annual exceedance probability.

b. Damage loss exceedance probabilities

Our primary interest is the damage losses caused by high winds and how they might increase in the future. HAZUS has a physical-damage model that is based on wind load and resistance of building types. The wind-induced pressure and windborne debris impacts are modeled, and damages are estimated in terms of failure of the building envelope. The damage model is coupled to a loss model that computes losses to a building using modeled building damage states together with empirical cost estimations for repair and replacement (Vickery et al. 2006). Loss estimates are a summation of direct property-damage loss and business-interruption loss, although losses from the former are typically an order of magnitude larger than losses from the latter.

The method is more flexible than the traditional wind speed–dependent loss curves because it allows the approach to be extended to model the effects of code changes and mitigation strategies on reduction in damage and loss. Moreover, economic damage loss is modeled separately from physical damage to a building, and the total loss is the sum of the economic loss plus the physical-damage loss by census tract. Uncertainty levels on the damage estimates are on the order of a factor of 2 (Schneider and Berman 2010). The uncertainty arises from incomplete scientific knowledge of hurricane-winds effects on buildings and facilities, simplifications needed for a comprehensive analysis, and incomplete/inaccurate inventories of the built environment and related economic and demographic data. In cases in which incomplete or inaccurate inventories of the built environment exist, the range of uncertainty may exceed a factor of 2 or more.

We focus on losses for the residential portion of the base, which is a U.S. Census–designated place with a 2000 census population of 8082. The tract numbers are

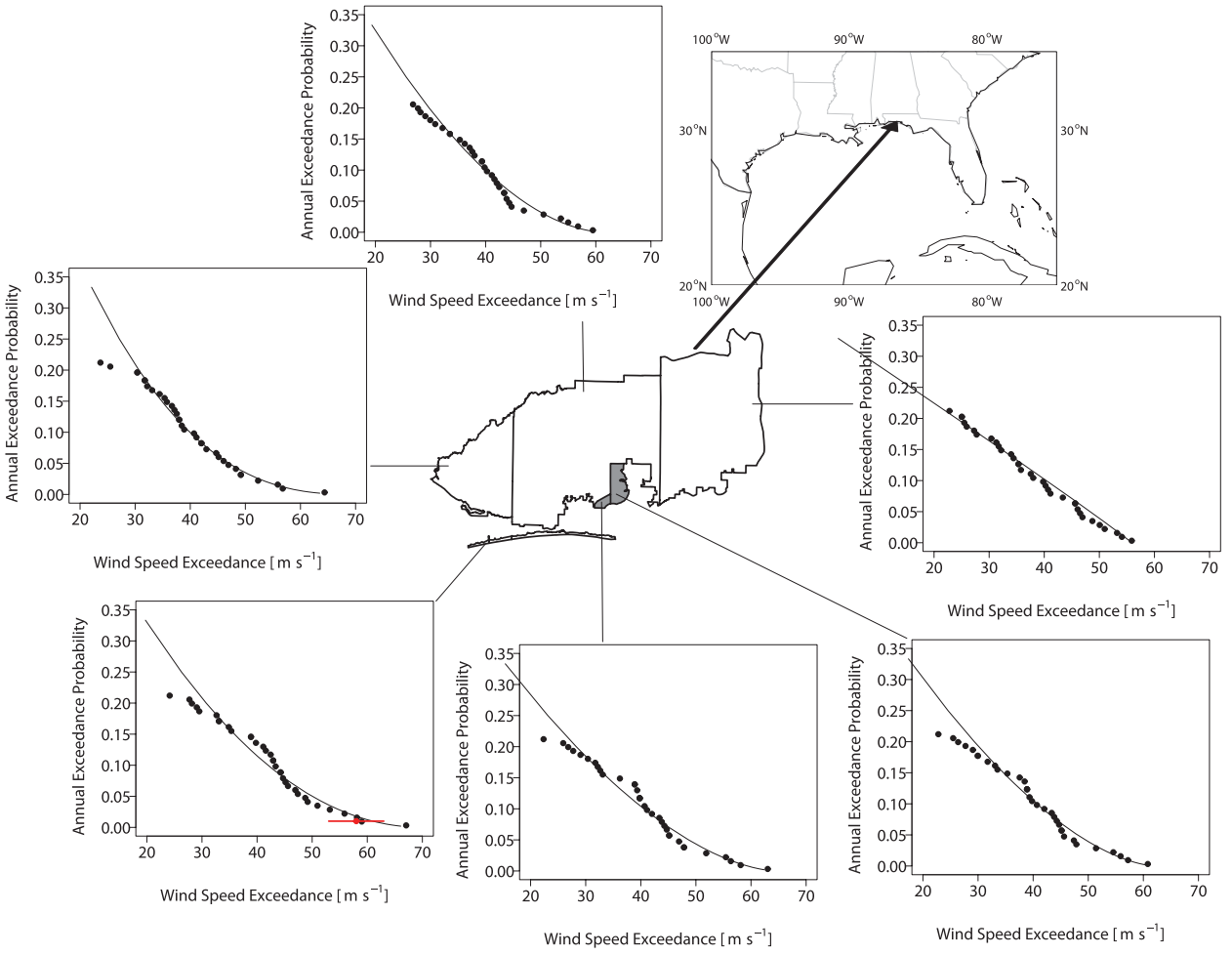

FIG. 3. Annual exceedance probabilities for hurricane wind speeds. The line represents a statistical model that is based on the method of POT. The empirical estimates are shown as points. The red point and line in the bottom-left panel (Santa Rosa Island) is the wind speed exceedance and 90% confidence interval that are based on the track-relative climatological model of Scheitlin et al. (2011). The two shaded census tracts correspond to where damage losses are estimated.

212 and 214. HAZUS estimates there are 4480 buildings in the region, which have an aggregate total replacement value of $717 million (in 2006 U.S. dollars). Approximately 80% of the buildings are residential, 11.5% are commercial, 5% are government, and 2% are industrial, with the remaining percentage divided among agricultural, religious, and education categories.

The loss estimates are based on aggregated type and floor-area inventories in each tract. The losses (repair, replacement, and business interruption) are normalized to 2006. So the interpretation of a $9 million loss estimate from Hurricane Eloise, which hit in 1975, is the loss expected for the exact same storm hitting the same location but with 2006 exposure levels. We model the set of wind-loss estimates using the same statistical method as was used for modeling wind speed. Losses are for nonmilitary buildings. Losses from military infrastructure require building-stock data that are substantially different from those used here.

The amount of damage increases sharply with increases in wind speed from a greater fraction of buildings failing and from a greater number of buildings suffering damage. Damage states in the model are defined as minor, moderate, severe, and complete destruction (failure), with the probability of each type increasing with increasing wind speed. For instance, a one-story, single-family, wood house exposed to a 54 m s^{-1} wind has a probability of failure of about 1%, a probability of severe damage of 5%, a probability of moderate damage of 32%, and a probability of minor damage of 85%. With a 60 m s^{-1} wind, these values increase to 5%, 25%, 65%, and 98%, respectively.

As an example, we compare the model-estimated damage losses between Hurricane Opal in 1995 and

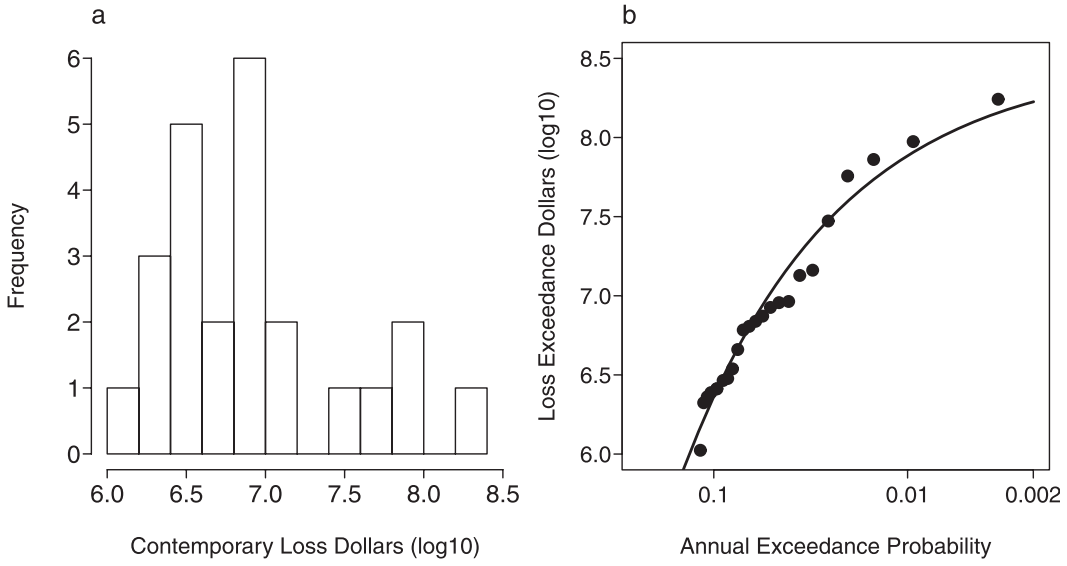

FIG. 4. Wind-damage losses from the set of historical hurricanes. (a) Histogram of the logarithm (base 10) of losses. (b) Annual exceedance probabilities for damage losses. The line represents a statistical model that is based on the method of POT. The losses are summed from the two census tracts composing the main EAFB (see Fig. 3).

Hurricane Dennis in 2005. Opal, which had a peak wind gust of 58 m s^{-1}, created moderate damage to 1350 (>30%) of the buildings. In contrast, Dennis, which had a peak wind gust of 41 m s^{-1}, created moderate damage to only 11 (<1%) of the buildings. The ratio of model-estimated residential damage to the total value of the residences for Opal is 94%, as compared with 4.4% for Dennis.

Figure 4 shows a histogram of wind-damage losses and a plot of the losses as a function of annual probability. The distribution is positively skewed even on the logarithmic scale (base 10). A value of 8 corresponds to a $100 million (M) loss. Loss amounts to the right of the distribution mode are of concern here. The largest loss, in excess of $174 M, occurred with the 1926 hurricane. We model losses exceeding $5 M with the model and empirical estimates shown in the right panel of Fig. 4. As with the wind speeds, the empirical estimates (points) are made using the inverse of the return rate. Because the points fall close to the curve, we are confident that the model provides a good summary of the data.

Again, because the loss exceedance curves are based on storminess over the past 160 yr, the annual probabilities are contemporary estimates. Next, we examine future loss exceedance curves after the hurricane wind speeds are statistically adjusted, with the magnitude of the adjustment being in accord with the Intergovernmental Panel on Climate Change (IPCC) estimates.

4. Changes in hurricane intensity

Recent research involving theory, models, and data provides the background for estimating possible future damage losses from hurricanes. For example, the heat-engine theory of tropical cyclone intensity argues for an increase in the maximum potential intensity of hurricanes with increases in sea surface temperature. Model projections that use scenario A1B from the IPCC Special Report on Emissions Scenarios indicate an increase in the frequency of average tropical cyclones of 2%–11% globally by the late twenty-first century, with the frequency of the most intense hurricanes likely increasing by a larger percentage (Knutson et al. 2010). Data analysis and modeling using a set of homogeneous tropical cyclone winds show that the strongest hurricanes are getting stronger—in particular, in the Gulf of Mexico and Caribbean Sea—with increases of as high as 20% per degree Celsius for the strongest hurricanes (Elsner and Jagger 2010). Here, we estimate future hurricane wind speeds and corresponding wind losses for EAFB. We begin by estimating the potential change in the strength of hurricanes over the Gulf of Mexico as Gulf water temperatures increase.

The first step is to estimate the potential influence of global warming on hurricane intensity. Knutson and Tuleya (2004) estimate an average 8% increase in hurricane intensity for every 1°C rise of SST on the basis of global tropical cyclone activity and for average hurricane intensity. Here, we examine evidence for hurricane

intensity increases over the Gulf of Mexico. We define the Gulf of Mexico as the region between 80° and 98°W longitude and between 19° and 32°N latitude. We choose all storms entering or developing within this domain over the period 1900–2009. The choice results in 450 storms. We eliminate the four storms having only a single 1-h position within the domain.

The SST data are the National Oceanic and Atmospheric Administration's reconstructed sea surface temperatures, version 3, (SST v3) from the Earth System Research Laboratory Physical Science Division and are available in network common data form (netCDF) format. NetCDF is a set of software libraries and machine-independent data formats that supports the creation, access, and sharing of array-oriented scientific data. We consider the July SST value averaged over the Gulf of Mexico region as an indicator of the heat content available for hurricanes during the peak season of August–October. Of the 39 hurricanes to affect EAFB, all occurred after 1 July and 32 occurred after 1 August. July SST is a reliable indicator of the amount of ocean heat available to hurricanes before the season begins.

We match the year of the July SST with the year of the per-storm maximum tropical cyclone intensity so that years with more than one tropical cyclone in the Gulf of Mexico will have the same July SST value. Using this dataset, we model the trend in tropical cyclone intensity as a function of SST using quantile regression. Quantile regression, introduced by Koenker and Bassett (1978), extends the ordinary least squares regression model to conditional quantiles (e.g., 90th percentile) of the response variable. Quantiles are points taken at regular intervals from the cumulative distribution function of a random variable. The quantiles mark a set of ordered data into equal-sized data subsets.

For example, of the 446 maximum-storm-intensity values in our Gulf of Mexico dataset, 25% of them are less than 22 m s^{-1} and 50% are less than 31 m s^{-1}. Thus, there is an equal number of tropical cyclones with intensities between 0 and 22 m s^{-1} as there is between 22 and 31 m s^{-1}. When we state that the median maximum intensity is 31 m s^{-1}, we mean that one-half of all cyclones have intensities of less than this value and one-half have intensities that are greater. In a similar way, the quartiles (deciles) divide the sample of intensities into 4 (10) groups with equal proportions of the sample in each group. The quantiles, or percentiles, refer to the general case.

Figure 5 shows the percent change in maximum tropical cyclone intensity with respect to a 1°C change in SST as a function of tropical cyclone intensity over the Gulf of Mexico using quantile regression (Elsner et al. 2008b; Jagger and Elsner 2009). To examine the possibility that biases in the early hurricane records will influence the results, we model the data first by using all storms since 1900 (Fig. 5, top panel) and then all storms since 1944. The points indicate the trend estimate computed from a quantile regression model for intensity quantiles from 0.01 to 0.99 by 0.01, and the vertical bar indicates 1 standard error about the estimate on the basis of the assumption of independent and identically distributed residuals, as is commonly used with normal linear regression. The nonlinear trend line is shown in red, and the 95% (nonsimultaneous) confidence band around this trend is shown in gray.

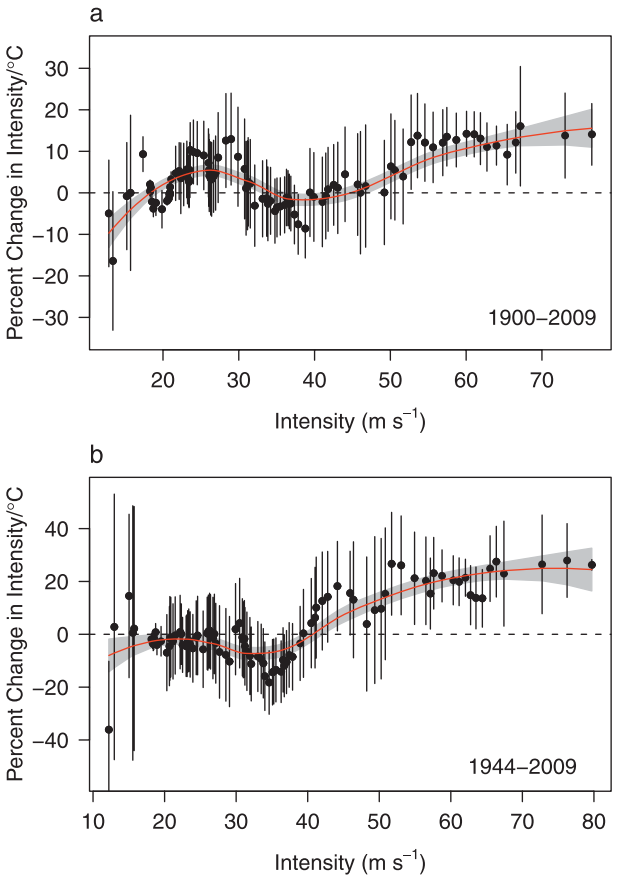

FIG. 5. Change in Gulf of Mexico tropical cyclone intensity. The change is modeled using data (a) from 1900 to 2009 and (b) from 1944 to 2009. The percentage change in intensity is with respect to a 1°C change in SST over the Gulf of Mexico and is a function of storm intensity. The dot and vertical line indicate the best estimate of the change and the 1 standard error. The red line is a local regression through the set of points, and the gray region defines the 95% confidence band on the trend.

The overall tendency is clear in showing little change in intensity for the weaker tropical cyclones but a large and, for some quantiles, statistically significant upward trend in intensity for the stronger tropical cyclones. The red line indicates a local polynomial regression fit through the points. The regression fit at intensity w is made using points in the neighborhood of w weighted by the distance from w.

The neighborhood size is set at a constant of 75% of the points. The nonlinear trend line does not change much when the early twentieth-century storms are removed, although the percentage increases are somewhat larger (note the change of scale on the vertical axis). In fact, the increase at the 90th-percentile storm intensity is 14% using storms dating back to 1900 as compared with 21% using storms only dating back to 1944.

It might be argued that the upward trend (as a function of SST) in the intensity of Gulf of Mexico tropical cyclones is not germane to the subset of those hurricanes affecting EAFB. To examine the case for this argument, we rerun the analysis on a smaller domain covering only the area from 85° to 95°W and from 25° to 32°N. This domain bounds the last 24 h of the historical hurricane tracks. We find a similar nonlinear trend in the percentage change as a function of intensity quantile, with an increase for the strongest hurricanes approaching 20%. The larger percentage increase might be related to the fact that the Loop Current, with its high ocean heat content, often exists in this region.

5. Upward trend in Gulf of Mexico sea surface temperature

Next, we quantify the trend in SST and get an estimate of the increase in Gulf warmth by the year 2100. Estimates of global SST increases by 2100 range from 1° to 3°C on the basis of numerical climate models. We take a similar approach as with hurricane intensity and examine the July SST data over the Gulf of Mexico and show how it is changing over time.

Figure 6 shows the time trend in Gulf of Mexico SST since 1900. The warming is pronounced and statistically significant. The trend estimate shown as the black line amounts to 0.68°C $(100\ \text{yr})^{-1}$. The significance can be seen by the 95% confidence band (between the two red lines). The magnitude of warming is consistent with reports of between 0.4° and 1.0°C $(100\ \text{yr})^{-1}$ for global tropical ocean warming (Deser et al. 2010).

Note that we do not necessarily expect an extrapolation (linear at that) to represent the future. Yet, the method provides a quantitative estimate of what Gulf of Mexico hurricanes might encounter in the twenty-second century that is consistent with estimates of anthropogenic global warming.

6. A model for hurricane intensities in the Gulf of Mexico to 2100

An estimate of the per-degree-Celsius SST increase in hurricane intensities (as a function of intensity), together with an estimate of the SST warming by 2100, allow us to estimate the increase in wind speeds for each historical hurricane. The assumption is that the set of historical hurricanes is a representative sample of the frequencies and intensities of future hurricanes but that the strongest hurricanes will be stronger as a result of the additional warmth in the Gulf of Mexico. The approach is similar to that used in Mousavi et al. (2010) to estimate the potential impact of hurricane intensification and sea level rise on coastal flooding, but here we use wind speed instead of central pressure deficit for the change in hurricane intensity.

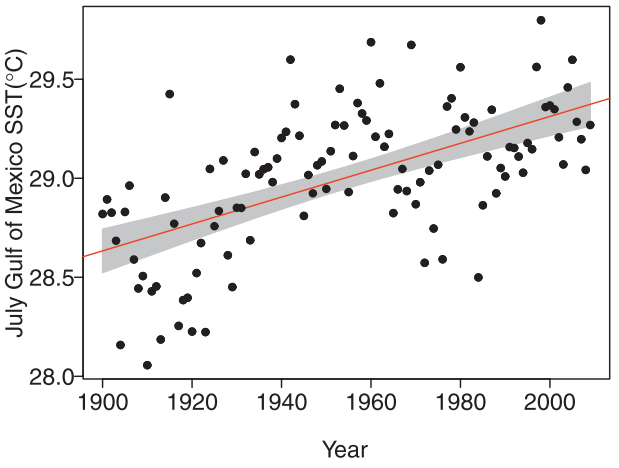

FIG. 6. Trend in Gulf of Mexico SST. The change in SST is the time trend over the past 110 yr. The points indicate the area-averaged SST value for July of each year over the period 1900–2009. The red line is the least squares regression line through the data, and the gray region defines the 95% confidence band on the trend.

Let w be the observed wind speed along the track of a historical hurricane; then the equation for w_{2100} representing the wind speed for the same hurricane in 2100 is given by

$$w_{2100} = [1 + \Delta w(w) \times \Delta\text{SST} \times 90]w, \qquad (1)$$

where $\Delta w(w)$ represents the fractional change in wind speed per degree-Celsius change in SST as a function of wind speed as described by the red curve in Fig. 5a; ΔSST represents the time trend in SST expressed per year; and 90 is the number of years.

Our model for intensities to 2100 is applied to wind speeds along the track for each historical hurricane affecting EAFB. Figure 7 shows the relationship between the historical tropical cyclone winds and the tropical cyclone winds in 2100. For the weaker winds the difference between historical and future speeds is very small, but for the strongest winds the future is windier. Each wind speed value in the historical dataset of hurricanes is transformed in such a way that the order is preserved. That is, if the wind speed was the 0.9 quantile

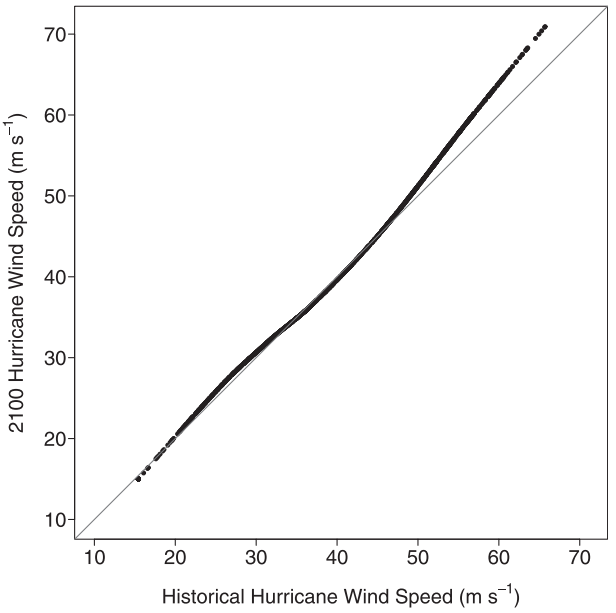

FIG. 7. Hurricane wind speeds (m s^{-1}) from historical hurricanes on the horizontal axis vs wind speeds from the same hurricanes occurring in 2100 on the vertical axis. Note the small change in the weaker wind speeds but the larger change (increase) in the strongest wind speeds.

in the historical dataset, it is the 0.9 quantile in the adjusted dataset but is transformed according to Eq. (1).

7. Future damage losses

The wind speeds along the track points are adjusted according to the model described in the previous section. However, the track-point locations and all other storm vitals remain the same because there is no observational, theoretical, or modeling evidence for changes to these storm characteristics in a warmer world. The new storm vitals are subsequently used by HAZUS to generate future loss estimates. We further assume (unrealistically) that there is no change in the number of buildings subjected to the increased winds, and all losses are expressed in 2006 dollars.

Table 2 shows the landfall wind speed, the peak gusts, and the wind-damage loss estimates for Eloise and a storm identical to Eloise occurring in 2100. The difference in landfall wind speed amounts to an increase of only 0.6%; the peak census-tract wind speed increases by 3.9%, however. This increase in wind speed results in a 45% increase in total wind-loss damage across the region. The amplification of wind speed increases by approximately an order of magnitude is higher than the factor-of-5 amplification that is based on historical hurricane winds and damage in the United States (Pielke et al. 2008). The greater damage might be a manifestation

TABLE 2. A comparison of Eloise and an analog of Eloise in 2100. The wind speed of the hurricane at landfall is given along with the peak gust over the two EAFB census tracts. The wind-damage losses in millions of dollars are output from the HAZUS model.

	Eloise (1975)	Eloise analog (2100)
Landfall W_{max} (m s^{-1})	46.6	46.9
Peak gust (m s^{-1})	45.6	47.4
Wind-damage losses ($M)	9.05	13.2

of the relative differences in housing construction for this part of Florida as compared with elsewhere, especially the Northeast.

Statistical models of loss estimates for contemporary and future hurricanes are compared in Fig. 8. The loss curve using the historical hurricanes (contemporary) is in black and is the same curve that was shown in Fig. 4b. All dollar amounts are normalized to 2006. The values are transformed to the common logarithm (log base 10) of dollar amounts. The loss curve from future hurricanes is in blue and is based on the wind speed model of the previous section. Both the contemporary and future loss models use a threshold of $5 million for the minimum loss event. No adjustment is made for future inflation, wealth, or building stock.

As expected, the probability of future losses is higher, but in particular for the largest loss events. For annual exceedance probabilities of less than 1 in 11 yr, future losses are projected to be greater than contemporary losses, assuming all else remains the same. The 90% confidence band around the percent increase is based on rerunning the loss model using winds estimated from the upper and lower values of the 95% confidence limits on the nonlinear trend line (Fig. 5) of wind speed as a function of SST and the upper and lower values of the 95% confidence limits on the trend in SST (Fig. 6). The results show that, if future projections of hurricane intensity are realized, coastal losses on the 1-in-100-yr (1 in 500 yr) storm will increase by 36% (52%) relative to today's losses, making EAFB more vulnerable to future losses from the strongest hurricanes.

8. Summary and model limitations

Hurricanes and tropical storms pose a significant natural threat to coastal military infrastructure. Here, we modeled contemporary and future wind speeds and damage losses from hurricanes affecting EAFB using statistical and dynamical models.

The results show that, if future extrapolations and projections of hurricane intensity are realized, coastal losses will increase for the strongest hurricanes by 36% [(13%, 76%) = 90% confidence interval] relative to

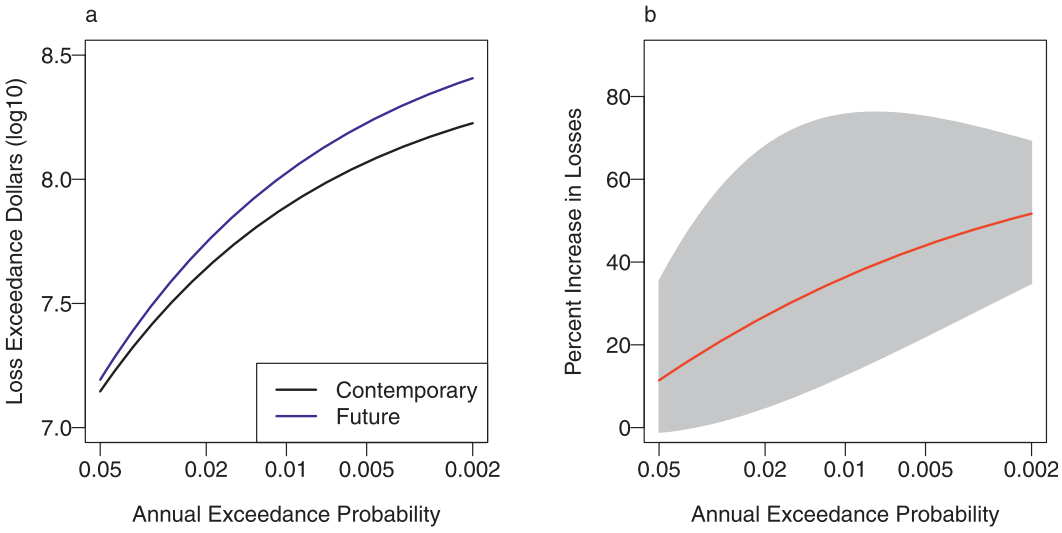

FIG. 8. Modeled loss curves and percentage increase in losses. (a) For the modeled loss curves, the black line represents loss exceedances that are based on the historical record of hurricanes affecting the two main census tracts in EAFB (contemporary losses) and the blue line represents loss exceedances that are based on our model for the same set of hurricanes but with intensities modeled on projected changes for storms in the Gulf of Mexico (future losses). (b) The percentage increase in losses displayed as a function of annual exceedance probability (log base-10 scale). The gray region defines the 90% confidence band that is based on the estimated uncertainty of the change in wind speed as a function of SST and on the uncertainty on the trend in SST.

today's losses, making EAFB progressively more vulnerable to hurricanes. The approach is important to the U.S. Air Force in terms of quantifying the possible risk in the coming years in light of potentially warmer SSTs and stronger tropical cyclone winds. The model compares changes in wind speed as a statistical function of temporal changes in SST rather than directly modeling temporal changes in wind speed.

Contemporary damage estimates are based on the record of past hurricanes. Although relying only on the relatively few historical events might lead to larger biases in assessing short-term risk (1–10 yr) when compared with the simulation method widely employed in the insurance business, it allows us to condition the long-term risk (greater than 50 yr) on a changing climate.

The estimated future losses depend on a number of assumptions that can be examined in more detail. In particular, our approach assumes a linear trend in SST. This is a reasonable fit for the historical data, but it might not be the case over the next 90 yr. Even with a linear trend, the rate of change, although consistent with global estimates and projections of SST, may be lower (or higher) than what is used here.

Also, Eq. (1) is conservative with respect to the uncertainty estimates because the change in SST is based on 90 yr but the historical storms all occur before 2010. We could instead use the prediction error for each storm and adjust the change in SST on the basis of the actual storm year. Moreover, the local regression smoother removes noise from the analysis, and therefore our confidence intervals are too small. A bootstrap over the entire model process would be a better way to estimate confidence bands.

Furthermore, the assumption that the incidence of hurricanes will be unchanged in the future might need to be modified. In fact, a recent study using numerical simulations indicates that the frequency of hurricanes across the Atlantic basin may decline in a warmer world (Knutson et al. 2008) although it is unclear as to what physical mechanism might cause such a decline.

More technical assumptions include the threshold parameter used in the extreme-value statistical model for losses, the value of the Holland *B* parameter, and the radius to maximum winds. Variations in these values will result in changes to our estimate of future losses. Our method represents an early attempt to quantify how much greater hurricane wind–related losses might be in the future, the above caveats notwithstanding. It will certainly be refined and improved.

Acknowledgments. The work was supported with a contract from the Strategic Environmental Research and Development Program (SERDP SI-1700). All statistical analyses were performed using the software environment R (http://www.r-project.org). We thank FEMA for the use of HAZUS and Frank Lavelle for

help with our questions about using it. We thank Robert E. Hodges for help with the SST data.

REFERENCES

Barnett, M. R., 2006: Hurricane Dennis & Hurricane Katrina: Final report on 2005 hurricane season impacts to northwest Florida. Florida Dept. of Environmental Protection Division of Water Resource Management Bureau of Beaches and Coastal Systems Rep., 122 pp. [Available online at http://bcs.dep.state.fl.us/reports/2005/2005hurr.pdf.]

Bender, M. A., T. R. Knutson, R. E. Tuleya, J. J. Sirutis, G. A. Vecchi, S. T. Garner, and I. M. Held, 2010: Modeled impact of anthropogenic warming on the frequency of intense Atlantic hurricanes. *Science,* **327,** 454–458.

Brown, D. P., J. L. Franklin, and C. Landsea, 2006: A fresh look at tropical cyclone pressure-wind relationships using recent reconnaissance based ''best-track'' data (1998–2005). Preprints, *27th Conf. on Hurricanes and Tropical Meteorology,* Orlando, FL, Amer. Meteor. Soc., 3B.5. [Available online at http://ams.confex.com/ams/pdfpapers/107190.pdf.]

Deser, C., A. S. Phillips, and M. A. Alexander, 2010: Twentieth century tropical sea surface temperature trends revisited. *Geophys. Res. Lett.,* **37,** L10701, doi:10.1029/2010GL043321.

Elsner, J. B., and T. H. Jagger, 2004: A hierarchical Bayesian approach to seasonal hurricane modeling. *J. Climate,* **17,** 2813–2827.

——, and ——, 2010: On the increasing intensity of the strongest Atlantic hurricanes. *Hurricanes and Climate Change,* Vol. 2, J. B. Elsner et al., Eds., Springer, 175–190.

——, ——, and K.-b. Liu, 2008a: Comparison of hurricane return levels using historical and geological records. *J. Appl. Meteor. Climatol.,* **47,** 368–374.

——, J. P. Kossin, and T. H. Jagger, 2008b: The increasing intensity of the strongest tropical cyclones. *Nature,* **455,** 92–95.

Holland, G. J., 1980: An analytical model of the wind and pressure profiles in hurricanes. *Mon. Wea. Rev.,* **108,** 1212–1218.

Jagger, T. H., and J. B. Elsner, 2006: Climatology models for extreme hurricane winds near the United States. *J. Climate,* **19,** 3220–3236.

——, and ——, 2009: Modeling tropical cyclone intensity with quantile regression. *Int. J. Climatol.,* **29,** 1351–1361.

Keim, B. D., R. A. Muller, and G. W. Stone, 2007: Spatiotemporal patterns and return periods of tropical storm and hurricane strikes from Texas to Maine. *J. Climate,* **20,** 3498–3509.

Khain, A., B. Lynn, and J. Dudhia, 2010: Aerosol effects on intensity of landfalling hurricanes as seen from simulations with the WRF model with spectral bin microphysics. *J. Atmos. Sci.,* **67,** 365–384.

Klotzbach, P. J., 2008: Refinements to Atlantic basin seasonal hurricane prediction from 1 December. *J. Geophys. Res.,* **113,** D17109, doi:10.1029/2008JD010047.

Knutson, T. R., and R. E. Tuleya, 2004: Impact of CO_2-induced warming on simulated hurricane intensity and precipitation: Sensitivity to the choice of climate model and convective parameterization. *J. Climate,* **17,** 3477–3495.

——, J. J. Sirutis, S. T. Garner, G. A. Vecchi, and I. M. Held, 2008: Simulated reduction in Atlantic hurricane frequency under twenty-first-century warming conditions. *Nat. Geosci.,* **1,** 359–364.

——, and Coauthors, 2010: Tropical cyclones and climate change. *Nat. Geosci.,* **3,** 157–163.

Koenker, R., and G. Bassett, 1978: Regression quantiles. *Econometrica,* **46,** 33–50.

Kossin, J. P., and S. J. Camargo, 2009: Hurricane track variability and secular potential intensity trends. *Climatic Change,* **97,** 329–337.

Landsea, C. W., and Coauthors, 2004: The Atlantic Hurricane Database Reanalysis Project: Documentation for the 1851–1910 alterations and additions to the HURDAT database. *Hurricanes and Typhoons: Past, Present, and Future,* R. Murnane and K. b. Liu, Eds., Columbia University Press, 177–221.

——, G. A. Vecchi, and L. Bengtsson, and T. R. Knutson, 2010: Impact of duration thresholds on Atlantic tropical cyclone counts. *J. Climate,* **23,** 2508–2519.

Malmstadt, J. C., K. N. Scheitlin, and J. B. Elsner, 2009: Florida hurricanes and damage costs. *Southeast. Geogr.,* **49,** 108–131.

——, J. B. Elsner, and T. H. Jagger, 2010: Risk of strong hurricane winds to Florida cities. *J. Appl. Meteor. Climatol.,* **49,** 2121–2132.

Mousavi, M. E., J. L. Irish, A. E. Frey, F. Olivera, and B. L. Edge, 2010: Global warming and hurricanes: The potential impact of hurricane intensification and sea level rise on coastal flooding. *Climatic Change,* **104,** 575–597.

Pielke, R. A., J. Gratz, C. W. Landsea, D. Collins, M. A. Saunders, and R. Musulin, 2008: Normalized hurricane damage in the United States: 1900–2005. *Nat. Hazards Rev.,* **9,** 29–42.

Powell, M. D., S. H. Houston, L. R. Amat, and N. Morisseau-Leroy, 1998: The HRD real-time hurricane wind analysis system. *J. Wind Eng. Ind. Aerodyn.,* **77-78,** 53–64.

Rappaport, E. N., J. L. Franklin, A. B. Schumacher, M. DeMaria, L. K. Shay, and E. J. Gibney, 2010: Tropical cyclone intensity change before U.S. Gulf Coast landfall. *Wea. Forecasting,* **25,** 1380–1396.

Scheitlin, K. N., J. B. Elsner, S. W. Lewers, J. C. Malmstadt, and T. H. Jagger, 2011: Risk assessment of hurricane winds for Eglin Air Force Base in northwestern Florida, USA. *Theor. Appl. Climatol.,* doi:10.1007/s00704-010-0386-4, in press.

Schneider, P., and E. Berman, 2010: Multi-hazard loss estimation methodology hurricane model—HAZUS-MH MR5 technical manual. Department of Homeland Security Federal Emergency Management Agency Mitigation Division Tech. Manual, 1014 pp. [Available online at http://www.fema.gov/library/file;jsessionid=315BA9DB4EF96B08ED5DB86B3BCDD820.WorkerLibrary?.]

Solow, A. R., 2010: On the maximum observed wind speed in a randomly sampled hurricane. *J. Climate,* **23,** 1262–1265.

Vecchi, G. A., and T. R. Knutson, 2008: On estimates of historical North Atlantic tropical cyclone activity. *J. Climate,* **21,** 3580–3600.

Vickery, P. J., and D. Wadhera, 2008: Statistical models of Holland pressure profile parameter and radius to maximum winds of hurricanes from flight-level pressure and H*Wind data. *J. Appl. Meteor. Climatol.,* **47,** 2497–2517.

——, J. Lin, P. F. Skerlj, L. A. Twisdale, and K. Huang, 2006: HAZUS-MH hurricane model methodology. I: Hurricane hazard, terrain, and wind load modeling. *Nat. Hazards Rev.,* **7,** 82–93.

——, F. J. Masters, M. D. Powell, and D. Wadhera, 2009a: Hurricane hazard modeling: The past, present, and future. *J. Wind Eng. Ind. Aerodyn.,* **97,** 392–405.

——, D. Wadhera, M. D. Powell, and Y. Chen, 2009b: A hurricane boundary layer and wind field model for use in engineering applications. *J. Appl. Meteor. Climatol.,* **48,** 381–405.